Simulations of Hierarchical Basis Reachability Graphs

Ziyue Ma, Guanghui Zhu, Zhiwu Li

October 6, 2019

In this note we report two benchmarks of *Hierarchical Basis Reachability Graphs* (HBRGs). Results are carried out on a laptop computer with Intel i5-4200M 2.5 GHz processor and 8 GB DDR3 1600Hz RAM.

1 Benchmark 1

The net in Figure 1 is slightly modified from Figure 5 in [1], a Petri net modeling a complex automatic manufacturing system. Comparing with the net in [1], two self-looped arcs ($t_{33} \leftrightarrow p_6$, $t_{36} \leftrightarrow p_{21}$) and one directed arcs ($t_{39} \rightarrow p_{46}$) are removed. This net contains 46 places and 39 transitions. The set of observable transitions contains 24 transitions:

$$T_o = \{t_1, t_3, t_6, t_7, t_8, t_9, t_{13}, t_{14}, t_{15}, t_{16}, t_{20}, t_{21}, t_{22}, t_{23}, t_{24}, t_{26}, t_{28}, t_{29}, t_{30}, t_{31}, t_{32}, t_{33}, t_{34}, t_{39}\}.$$

The initial marking shown in the figure is parameterized as: $M_0 = a \cdot p_1 + b \cdot p_{16} + p_{31} + p_{32} + p_{33} + p_{34} + p_{35} + p_{37} + p_{38} + p_{39} + 8p_{40} + p_{41}$.

1.1 Hierarchical Partition I

Consider a hierarchical partition $T_o = T_{pri} \cup T_{sec}$ where the primary observable transitions (marked in blue in Figure 1) are:

$$T_{pri} = \{t_1, t_6, t_7, t_9, t_{13}, t_{14}, t_{20}, t_{21}, t_{23}, t_{26}, t_{29}, t_{31}, t_{34}\}$$

and the secondary observable transitions (marked in red in Figure 1) are:

$$T_{sec} = \{t_3, t_8, t_{15}, t_{16}, t_{22}, t_{24}, t_{28}, t_{30}, t_{32}, t_{33}, t_{39}\}.$$

The simulation results for computing BRGs (with respect to $T_E = T_o$) and HBRGs are summarized in Table 1. One can see that when the initial marking is not so small (entries 3 to 8), the size of an HBRG is less than 15% of that of the RG: such a ratio is continuously decreasing when the size of RG increases. Although the size of an HBRG is about twice as large as that of the corresponding BRG, the time consumption to compute an HBRG is only about 5% of that to compute the BRG.

a	b	RG	BRG	τ_B	HBRG	τ_H	HBRG/RG	τ_H/τ_B
1	1	1966	680	0.081	849	0.033	43.1%	40.7%
1	2	12577	3180	0.374	4447	0.189	35.3%	50.5%
1	3	44942	8828	2.127	13051	0.304	29.0%	14.2%
2	2	76808	13214	5.242	19469	0.397	25.3%	7.5%
2	3	262236	35498	83.587	53695	1.388	20.4%	1.6%
2	4	586604	68114	264.434	103504	2.342	17.6%	0.8%
3	3	853850	87038	379.398	133286	3.516	15.6%	0.9%
3	4	1837329	163470	1090.782	248119	10.758	13.5%	0.9%

Table 1: Simulations results of Benchmark 1.1 with different values of a and b. RG, BRG, and HBRG denote the numbers of markings/nodes in the reachability graph, BRG, and HBRG, respectively. τ_B and τ_H are time-consumptions (in *seconds*) to compute BRG and HBRG, respectively.

1.2 Hierarchical Partition II

Consider the same net but a different hierarchical partition $T_o = T_{pri} \cup T_{sec}$ where the primary observable transitions are:

$$T_{pri} = \{t_3, t_6, t_8, t_9, t_{13}, t_{15}, t_{16}, t_{20}, t_{22}, t_{24}, t_{28}, t_{29}, t_{31}, t_{34}\}$$

and the secondary observable transitions are:

$$T_{sec} = \{t_1, t_7, t_{14}, t_{21}, t_{23}, t_{26}, t_{30}, t_{32}, t_{35}, t_{39}\}.$$

Transitions in sets T_{pri} and T_{sec} are marked in blue and red, respectively, in Figure 2. The simulation results for computing BRGs (with respect to $T_E = T_o$) and HBRGs are summarized in Table 2.

a	b	RG	BRG	τ_B	HBRG	τ_H	HBRG/RG	τ_H/τ_B
1	1	1966	680	0.092	720	0.041	36.6%	16.3%
1	2	12577	3180	0.414	3720	0.087	29.5%	8.2%
1	3	44942	8828	2.250	10924	0.245	24.3%	2.0%
2	2	76808	13214	6.668	16914	0.519	22.0%	1.7%
2	3	262236	35498	80.886	48184	2.474	18.3%	0.2%
2	4	586604	68114	283.270	95714	9.203	16.3%	0.1%
3	3	853850	87038	402.530	122576	14.235	14.3%	0.1%
3	4	1837329	163470	1206.431	238450	51.174	12.9%	0.2%

Table 2: Simulations results of Benchmark 1.2 with different values of a and b. RG, BRG, and HBRG denote the numbers of markings/nodes in the reachability graph, BRG, and HBRG, respectively. τ_B and τ_H are time-consumptions (in *seconds*) to compute BRG and HBRG, respectively.

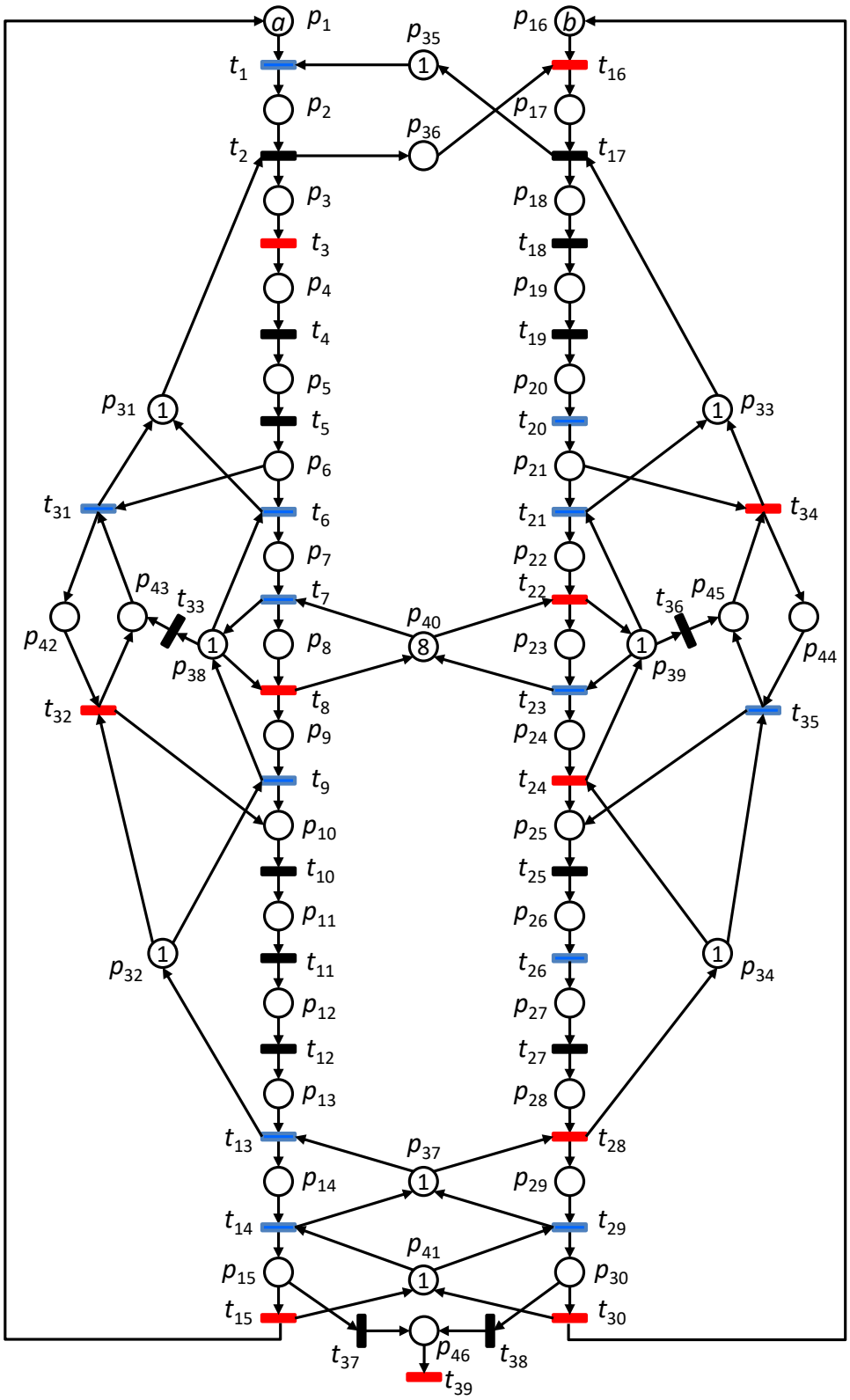

Figure 1: Benchmark 1.1. Sets $T_{pri} = \{t_1, t_6, t_7, t_9, t_{13}, t_{14}, t_{20}, t_{21}, t_{23}, t_{26}, t_{29}, t_{31}, t_{34}\}$ (blue), $T_{sec} = \{t_3, t_8, t_{15}, t_{16}, t_{22}, t_{24}, t_{28}, t_{30}, t_{32}, t_{33}, t_{39}\}$ (red).

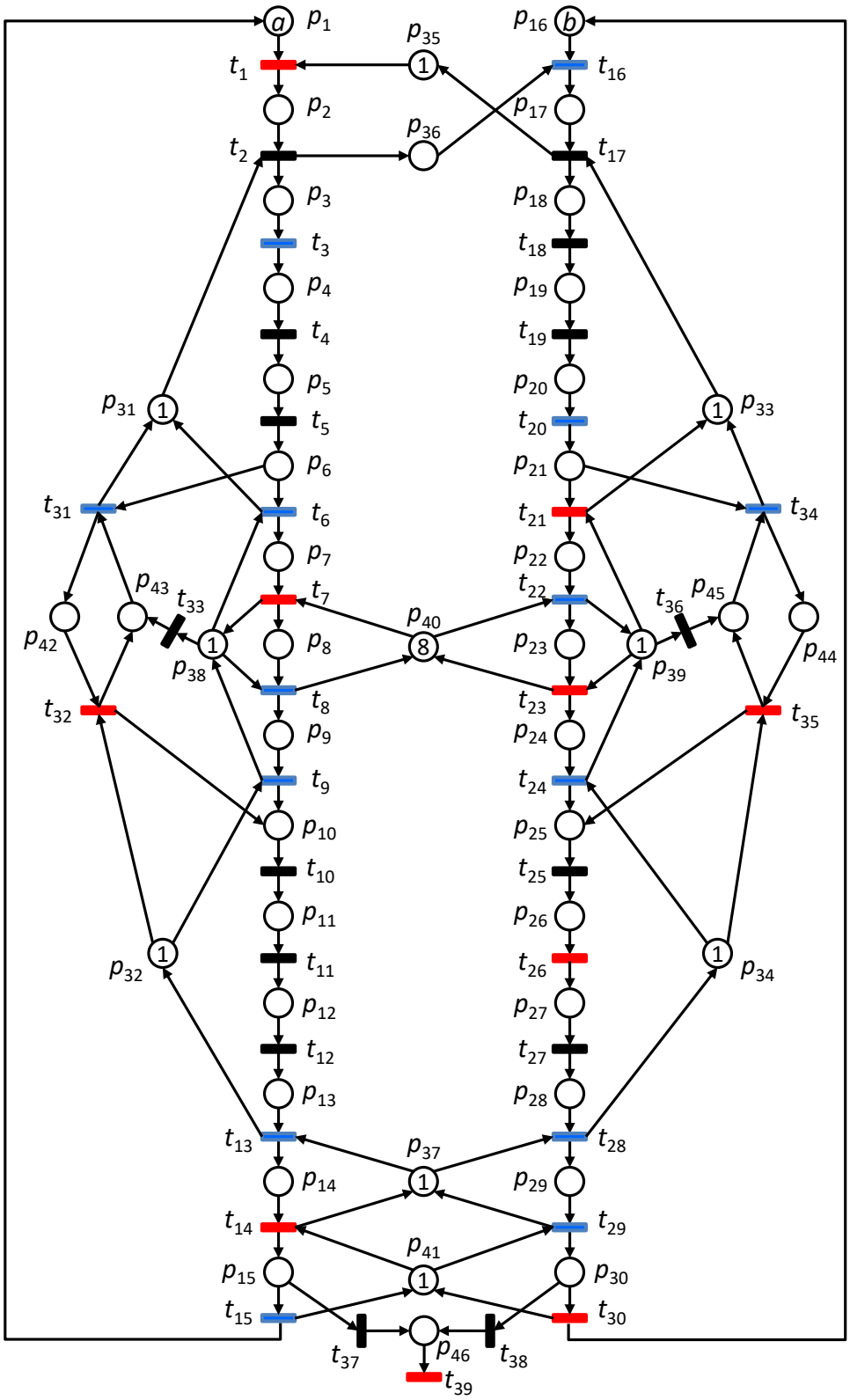

Figure 2: Benchmark 1.2. Sets $T_{pri} = \{t_3, t_6, t_8, t_9, t_{13}, t_{15}, t_{16}, t_{20}, t_{22}, t_{24}, t_{28}, t_{29}, t_{31}, t_{34}\}$ (blue), $T_{sec} = \{t_1, t_7, t_{14}, t_{21}, t_{23}, t_{26}, t_{30}, t_{32}, t_{35}, t_{39}\}$ (red).

2 Benchmark 2

The net in Figure 3 is taken from [2] which models a series of parallel work-flows. This net has three parameters: the number of work-flows (as well as the weight from p_1 to t_1) n, the length of each work-flows m, and the initial number of tokens $M_0(p_1) = a$. The set $T_o = T_{pri} \cup T_{sec}$, where the set T_{pri} (marked in blue) is parameterized as:

$$T_{pri} = \{t'_{km+1} \mid k = 1, \ldots, n\} \cup \{t''_{km+1} \mid k = 1, \ldots, n\}$$

and the set T_{sec} (marked in red) is parameterized as:

$$T_{sec} = \{t'_{k1} \mid k = 1, \ldots, n-1\} \cup \{t'_{km} \mid k = 2, \ldots, n\} \cup \{t''_{km} \mid k = 2, \ldots, n\}.$$

The simulation results of the BRGs (with respect to $T_E = T_o$) and HBRGs for different (n, m, a)'s are summarized in Table 3. In this simulation, the size of HBRG is slightly larger than the size of a BRG, but the time consumption to compute an HBRG is much smaller, especially in the case where the size of RG and BRG is large (the last two entries).

n	m	a	RG	BRG	τ_B	HBRG	τ_H	HBRG/RG	τ_H/τ_B
2	1	4	121	81	0.005	81	0.002	66.9%	40.0%
2	2	4	361	108	0.008	81	0.001	22.4%	12.5%
2	3	4	841	108	0.011	81	0.003	9.6%	27.2%
2	1	6	1648	1323	0.101	1323	0.008	80.2%	7.9%
2	2	6	9460	2106	0.192	1323	0.017	13.9%	8.8%
2	3	6	36205	2106	0.193	1323	0.015	3.6%	7.7%
3	1	6	2025	486	0.041	486	0.005	24.0%	12.1%
3	2	6	10000	648	0.068	648	0.011	6.4%	16.1%
3	3	6	34225	648	0.112	648	0.009	1.8%	8.0%
3	1	9	126905	40095	47.314	40095	0.346	31.6%	7.3%
3	2	9	1764787	65232	155.594	65232	0.605	3.7%	0.4%
3	3	9	13168689	65232	173.731	65232	0.690	0.5%	0.4%

Table 3: Simulations results of Benchmark 2 with different values of n, m, a.

References

[1] M. Cabasino, A. Giua, M. Pocci, and C. Seatzu, "Discrete event diagnosis using labeled Petri nets: an application to manufacturing systems," *Control Engineering Practice*, vol. 19, no. 9, pp. 989–1001, 2011.

[2] M. P. Cabasino, A. Giua, L. Marcias, and C. Seatzu, "A comparison among tools for the diagnosability of discrete event systems," in *Proceedings of the 2012 IEEE International Conference on Automation Science and Engineering*, Aug 2012, pp. 218–223.

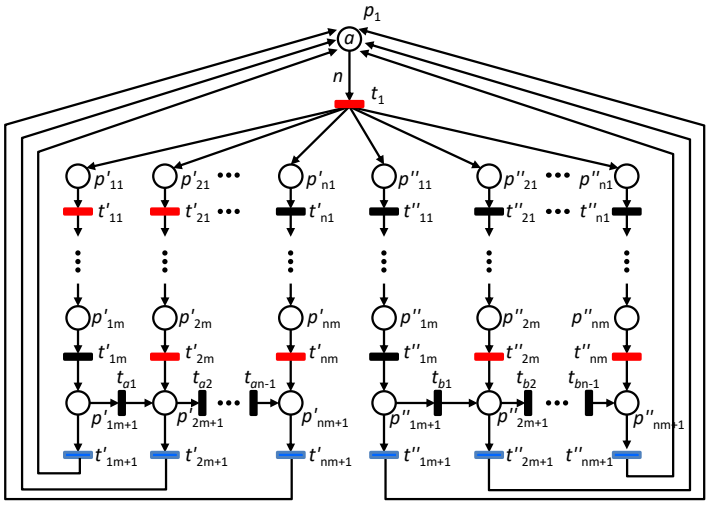

Figure 3: Benchmark 2. Transitions in sets T_{pri} and T_{sec} are marked in blue and red, respectively.